Tectonophysics 514–517 (2012) 146–155

Contents lists available at SciVerse ScienceDirect

Tectonophysics

journal homepage: www.elsevier.com/locate/tecto

Initiation of Rayleigh–Taylor instabilities in intra-cratonic settings

Weronika Gorczyk [a,*], Bruce Hobbs [a,b], Taras Gerya [c]

[a] University of Western Australia (UWA), Australia
[b] Australian Commonwealth Scientific and Research Organisation (CSIRO), Australia
[c] Swiss Federal Institute of Technology Zürich (ETHZ), Switzerland

ARTICLE INFO

Article history:
Received 4 October 2010
Received in revised form 17 October 2011
Accepted 18 October 2011
Available online 25 October 2011

Keywords:
Intra-plate deformation
Rayleigh–Taylor instability
Numerical modelling
Lithosphere

ABSTRACT

A new model of instability development in the lithosphere is presented whereby Rayleigh–Taylor instabilities are initiated as a result of heterogeneities in plastic strength within the lithosphere. Such a model does not depend on large initial variations in the thickness or density of the lithosphere for instabilities to form and hence differs from previously proposed mechanisms. The model is particularly relevant to intra-plate orogenic processes and reproduces many aspects of structural and metamorphic events observed in such settings. In particular the surface topographic evolution of intra-plate settings, especially the development of large intracratonic basins, is reproduced. The application to processes operating in an intra-cratonic setting at old cratonic margins is discussed.

1. Introduction

Although the concept of plate tectonics has revolutionised our understanding of many processes associated with plate boundaries, there is still limited understanding of the dynamics of intra-plate deformation. Though the large-scale tectonic deformation of the lithosphere is mostly confined to plate boundary regions, significant deformation can also occur in plate interiors (i.e.: Begg et al., 2009; Calais et al., 2005; Calais et al., 2006; Craddock and van der Pluijm, 1999; Stephenson et al., 2009). Continental plates contain sedimentary basins, including intra-plate basins developed far from plate margins (i.e.:Ingersoll, 1988; Kevin, 1976; Sandiford et al., 2009; Ye et al., 1985). Similarly, episodes of intraplate crustal uplift and orogeny are evident in the geological record (Buick et al., 2001; Dyksterhuis and Muller, 2008; Sandiford and Hand, 1998). The tectonic evolution of these intraplate features must either be caused by forces transmitted through the lithosphere from plate boundaries or by some other so far poorly-defined or unknown mechanism. A mechanism that is at least spatially independent of plate boundaries is dynamic interaction between the lithosphere and underlying mantle, which leads to the mechanical removal of portions of mantle lithosphere. Two of the primary removal mechanisms that have been put forward include: (1) *delamination* (Fig. 1a), a wholesale peeling away of a coherent block of the mantle lithosphere, and (2) lithospheric "dripping", initiated by a *Rayleigh–Taylor instability* (Figs. 1b, 2) of the viscous mantle lithosphere. These mantle lithospheric removal events are commonly based on processes involving density contrasts between the mantle lithosphere and the less dense underlying mantle. Such density contrasts can arise as a result of thermal contraction of the cold mantle lithosphere, although compositional density variations of the lower crust have also been called upon to explain the initiation of lithospheric instabilities (Jull and Kelemen, 2001).

Bird (1978, 1979) proposed a model of mantle lithosphere delamination, where the cold and dense mantle lithosphere peels away as a coherent slice from the crust along the Moho, for example, a brittle oceanic plate falls away from beneath a collisional orogen. The removed slice of mantle lithosphere is replaced by underlying hot and buoyant asthenosphere. Generally, this form of delamination is predicated on the idea that the hot-weak lower crust is the most pronounced strength-jump layer in the lithosphere. This results in separation between the strong crust and strong mantle lithosphere portions of the plate.

A second hypothesis explains loss of the lower lithosphere in a ductile manner, due to gravitational instability. Some authors call this process convective removal due to negative thermal buoyancy of the cold lithosphere (i.e.: Conrad and Molnar, 1999; Houseman and McKenzie, 1982), while others (i.e.:Elkins-Tanton, 2007; Hoogenboom and Houseman, 2006; Neil and Houseman, 1999) ascribe this process as Rayleigh–Taylor instability due to density variation between asthenosphere and mantle lithosphere. This mechanism requires no specific structural weakness beyond a thickened region in the lithosphere that is gravitationally unstable with respect to the underlying mantle and that possesses a rheology conducive to flow (Elkins-Tanton and Hager, 2000; Schott and Schmeling, 1998).

The explicit assumption of the convective removal is that there is sufficient perturbation (and at a suitable wavelength) within the

* Corresponding author.
E-mail address: weronika.gorczyk@gmail.com (W. Gorczyk).

0040-1951/$ – see front matter © 2011 Elsevier B.V. All rights reserved.
doi:10.1016/j.tecto.2011.10.016

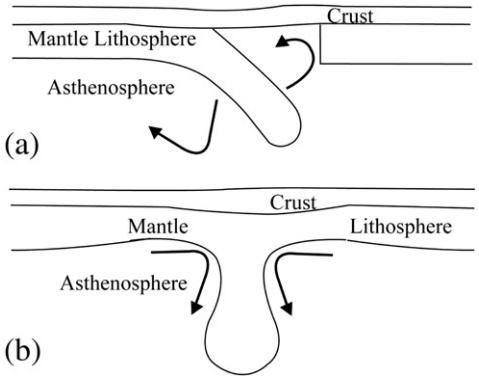

Fig. 1. Schematic illustration of geodynamic models for mantle lithosphere removal. (A) Delamination of the mantle lithosphere after Bird (1979). (B) Rayleigh–Taylor instability — gravitational instability of the mantle lithosphere after Houseman et al. (1981).

mantle lithosphere to initiate the Rayleigh–Taylor instability. Furthermore, the growth rate of the instability must outpace the thermal diffusion of the cold mantle lithosphere root into the hot mantle so that the unstable region remains weak.

In this paper we first summarise previous studies on the development of the Rayleigh–Taylor instability as a topographic response with associated magmatic activity. Then we raise and address a fundamental question: *How are such instabilities triggered in intraplate settings, without the involvement of relatively large topographic perturbations at the base of the crust or lithosphere and without density contrasts between the lithosphere and asthenosphere*? This leads to another key question: *How is mechanical thickening initiated in intra-plate regions far form plate boundaries*?

2. Numerical approach

To simulate dynamic development of the Rayleigh–Taylor instabilities, the 2D code I2ELVIS (Gerya, 2010; Gerya and Yuen, 2007) is used. It combines a conservative finite difference method with non-diffusive marker-in-cell techniques. In the model visco-elasto-plastic rheology of the rocks (Ranalli, 1995) is used.

Mechanical properties of the rocks used in the models are presented in Table 1. The effective creep viscosities of rocks are represented as a function of temperature and stress by experimentally determined flow laws. Viscosity for dislocation creep depending on strain rate, pressure and temperature is defined in terms of deformation invariants as (Elliott et al., 1997; Hawkesworth et al., 1997):

$$\eta_{creep} = (\dot{\varepsilon})^{(1-n)/n} F (A_D)^{-1/n} \exp\left(\frac{E+VP}{nRT}\right) \quad (1)$$

where $\dot{\varepsilon}_{II} = \sqrt{\frac{1}{2}\dot{\varepsilon}_{ij}\dot{\varepsilon}_{ij}}$ is the second invariant of the strain-rate tensor, and A_D, E, V and n are experimentally determined flow law parameters (Table 1), respectively material constant, activation energy, activation volume and stress exponent. F is a dimensionless coefficient depending on the type of experiments, upon which the flow law is based and used for conversion of experimentally determined rheology to model stress states. The plastic strength of a rock is determined as:

$$\sigma_{creep} = c + P \sin(\varphi), \quad (2)$$

$$\sin(\varphi) = \sin\left(\varphi_{dry}\right)\lambda_{fluid}, \quad (3)$$

where c is the cohesion, φ is the effective angle of an internal friction (φ_{dry} is φ for dry rocks), P is the dynamic pressure, and $\lambda_{fluid} = 1\text{-}P_{fluid}/P$ is the pore fluid pressure factor. The pore fluid pressure P_{fluid} reduces the yield strength σ_{yield} of fluid-containing porous or fractured media. For dry crystalline rocks, $\sin(\varphi)$ typically varies from 0.2 to 0.9, depending on pressure, temperature, and mineralogical compositions (Brace and Kohlstedt, 1980; Moore et al., 1997). After Gerya et al. (2008), we use high plastic strength of dry mantle ($\sin(\varphi) = 0.6$) and low plastic strength of hydrated rocks ($\sin(\varphi) = 0$–0.3, Table 1).

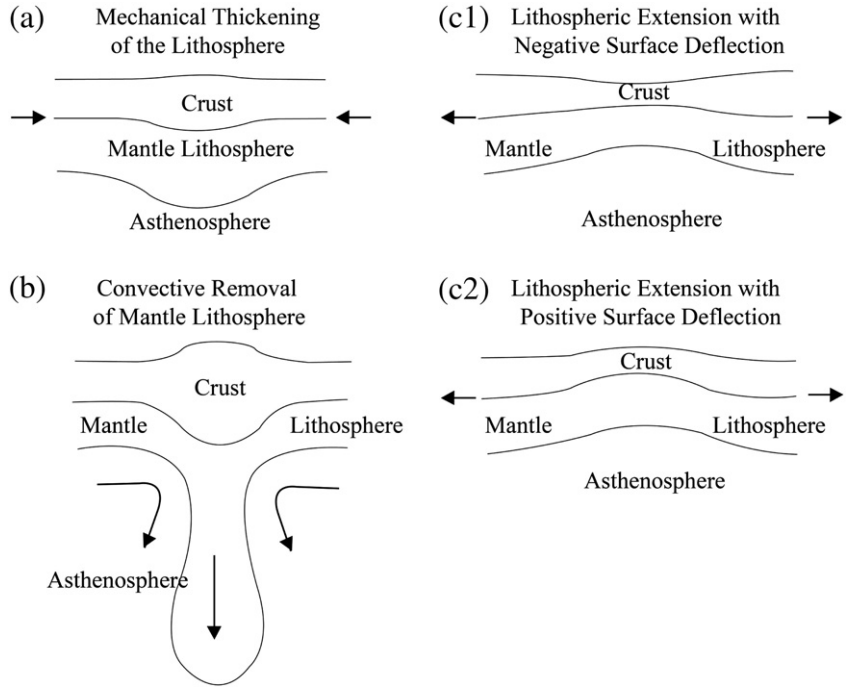

Fig. 2. Cartoon showing: (a) horizontal shortening and thickening of the continental crust and mantle lithosphere; (b) removal of mantle lithosphere and its replacement by hot asthenosphere that could result in rapid uplift at the surface; (c1) collapse of the topography caused by lithospheric extension; (c2) topographic uplift during lithospheric extension (also observed in Elkins-Tanton, 2007).

Table 1
Material properties used in 2D numerical experiments. Q_L – latent heat; Hr – radiogenic heating; E – activation energy; n – stress exponent; A_D – material constant; V – activation volume; C – cohesion; Φ – friction angle; Cp = 1000 J kg^{-1} K^{-1}, $\alpha = 3\times10^{-5}$ K^{-1}, $\beta = 1\times10^{-5}$ MPa^{-1} for all rock types. 1 = (Turcotte and Schubert, 2002); 2 = (Bittner and Schmeling, 1995); 3 = (Clauser and Huenges, 1995); 4 = (Schmidt and Poli, 1998); 5 = (Ranalli, 1995 and references therein).
6 = (Gerya et al., 2008).

Material	ρ_0	k	Tsolidus	Tliquidus	Q_L	Hr	Flow	E	n	A_D	V	C	sin(φ)
	kg/m^3	W(m K)	K	K	kJ/kg	μWm^3	law,	kJ/mol		MPa^{-n}s^{-1}	J/(MPa·mol)	MPa	
Continental upper crust, sediments	2800 (solid) 2500 (molten)	[0.64 + 807/(T + 77)] × exp (0.00004 PMPa)	889 + 17900/(P + 54) + 20200/(P + 54)^2 at P < 1200 MPa, 831 + 0.06 P at P > 1200 MPa	1262 + 0.09P	300	1.0–5.0	Wet/dry quartzite	154	2.3	$10^{-3.5}$	0	3 1(for weak zone)	0.15 0.1(for weak zone)
Continental lower crust	3000 (solid) 2900 (molten)	[1.18 + 474/(TK + 77)] × exp (0.00004 PMPa)	973 − 70,400/(P + 354) + 77,800,000/(P + 354)^2 at P > 1600 MPa, 935 + 0.0035 P + 0.0000062 P^2 at P < 1600 MPa	1423 + 0.105P	380	0.25	Plagioclase An75	238	3.2	$10^{-3.5}$	0	3 1(for weak zone)	0.4 0.15(for weak zone)
Lithosphere– asthenosphere dry mantle	3300	[0.73 + 1293/(TK + 77)] × exp (0.00004 PMPa)				0.022	Dry olivine	532	3.5	$10^{4.4}$	8	3	0.6 0.15(for weak zone)
References	1, 2	3	4	4	1, 2	1	5	5	5	5	1, 5	6	6

Two models are presented in this paper — spontaneous development of the Rayleigh–Taylor instabilities with an initial perturbation (Model 1) and thickening of the lithosphere (Model 2).

2.1. Initial and boundary condition

2.1.1. Model 1

The model spatial coordinate frame is 2000 × 300 km, and the initial geometry of the model corresponds to thickened intra-continental mantle lithosphere with and without a continental root (Fig. 3a1, b1). In this model continental crust consists of (1) 20 km of upper continental crust, (2) 20 km of lower continental crust and is underlain by (3) 40 km of continental mantle lithosphere (bulk rock properties are listed in Table 1). The subjacent mantle and mantle lithosphere is considered to be anhydrous peridotite. The topographic perturbation at the base of the lithosphere is imposed at the beginning of the simulation to allow for spontaneous development of deformation during the run, without the need for horizontal shortening forces. Free slip conditions are implemented at all boundaries except for the model bottom, which is free to move in both downwards and upwards directions (Gorczyk et al., 2007). Infinite-like external free slip conditions along the bottom imply free slip at 1200 km depth. Similar to the usual free slip condition, external free slip allows global conservation of mass in the computational domain.

2.1.2. Model 2

The model spatial coordinate frame is 1000 × 200 km. Continental crust consists of (1) 17 km of upper continental crust, (2) 18 km of lower continental crust and is underlain by (3) 45 km of continental mantle lithosphere (bulk rock properties are listed in Table 1). The boundary conditions are the same as in the previous model. The compression regime is prescribed by imposing locally constant velocities at 150 km $V_x = 1$ cm/yr and 850 km $V_x = -1$ cm/yr. The weak zone is prescribed with a lower plastic strength with respect to the surrounding rocks.

2.1.3. Partial melting

The stable mineralogy for each lithology is obtained by free energy minimization (Christensen and Yuen, 1985) as a function of pressure and temperature from thermodynamic data. For this purpose, phase relations were resolved on a grid with a resolution of 5 K and 25 MPa. Examples of phase diagrams computed for different lithologies are discussed by Connolly and Kerrick (2002) and Kerrick and Connolly (2002).

2.1.4. Topography

Above the continental crust, there is a 10 km thick low viscosity layer ($\eta = 10^{18}$ Pa·s) consisting of atmosphere ($\rho = 1$ kg/m^3). High contrast in viscosity between the upper weak layer and the crust causes minimal shear stress (<10^4 Pa) along the erosion/sedimentation surface (Burg and Gerya, 2005). Test experiments have shown that choosing lower viscosities of the weak layer do not affect notably the development of the topography.

The position of the surface of the crust is dynamically calculated as a free surface and changes spontaneously as it is affected be erosion and sedimentation processes specified by the transport equation, solved at every time-step on the Eulerian coordinates:

$$\frac{\partial y_{es}}{\partial t} = v_y - v_x \frac{\partial y_{es}}{\partial x} - v_s + v_e. \quad (4)$$

Where y_{es} is vertical position of the surface a function of the horizontal distance; v_y and v_x are the vertical and horizontal components of the material velocity vector at the surface, y is positive downwards,

$y=0$ at the top of the calculation domain); v_s and v_e are the sedimentation and erosion rates respectively, in the relation:

$$\begin{array}{llll} v_s = 0mm/a & v_e = 0.09mm/a & for & y<10km \\ v_s = 0.09mm/a & v_e = 0mm/a & for & y<11km \end{array}.$$

The increased sedimentation rates $v_s = 1mm/a$ accounts for slope instabilities in regions with steep slopes.

3. Initiation of the classical Rayleigh–Taylor instability

The classical model for the Rayleigh–Taylor instability and dripping of mantle lithosphere proposes a regime as the first stage (Fig. 2a), which is induced by horizontal compression and leads to mechanical shortening and thickening of the lithosphere. This is followed by detachment of the lower portion of mantle lithosphere and its replacement with hot asthenospheric mantle (Fig. 2b). This process leads to extension in the crust, which may be followed by surface subsidence (Houseman and Molnar, 1997, Fig. 1-c1), or uplift (Elkins-Tanton and Hager, 2000, Fig. 2(c2)). Further in this paper we refer to this process as "delamination" even though the term is also used in the literature to refer to peeling off part of the mantle lithosphere away.

Earlier investigations of the Rayleigh–Taylor instability in this context (i. e.: Conrad, 2000; Houseman and Molnar, 1997; Molnar et al., 1998) have explored the effects of various density, viscosity, anisotropy and temperature structures on the growth rate of the instability. These authors established the possibility that the process of delamination of the lower part of mantle lithosphere could occur within a period of time less than 20 million years. This time scale of fast delamination reduces significantly the influence of thermal diffusivity that can stabilize the layer over longer periods and prevent dripping. In these approaches the driving force for the lithospheric mantle removal is the variation in buoyancy of the unstable layer, in this case between the mantle lithosphere and asthenosphere. Several studies proposed that the lithosphere has a heterogeneous chemical composition, and this could make some parts of the lithosphere less buoyant than the asthenosphere (Anderson, 1995; Jordan, 1978; Poudjom Djomani et al., 2001). Elkins-Tanton (2007) and Kay and Kay (1993) suggested that phase changes in the deepest regions of lithospheric roots may contribute to the initiation of density instabilities. As the lithospheric root is depressed and enters the eclogite stability field, it becomes denser than the underlying asthenosphere due to phase changes. Schott and Schmeling (1998) concluded that a lithospheric root must be at least 100 to 170 km deep to create the negative buoyancy necessary for delamination. Lev and Hager (2008) suggested that anisotropic viscosities are strongly connected with lithospheric instabilities and have significant influence on development of Rayleigh–Taylor instabilities.

Piriz et al. (2009) analysed the stability of an elastic–plastic plate with respect to the formation of the Rayleigh–Taylor instabilities and showed that the transition from plastic stability to instability is given by:

$$\rho g \xi_o / \sqrt{3Y} = 1 - \sqrt{\rho g \lambda / 4\pi\mu} \quad (5)$$

where ρ is the density, g is the acceleration due to gravity, ξ_o is the magnitude of the initial perturbation at the base of the plate, λ is the wavelength of this perturbation and μ is the elastic shear modulus. If we take $\mu = 6.5^{10}$ Pa, $\rho = 3300$ kg m^{-3}, $\lambda = 10$ km and $Y = 1.0^9$ Pa then $\xi_o = 1.6$ m. Thus, if the Piriz analysis is applicable to the situation examined here then a plastic weakness of 10 km is always unstable given a small deflection and Rayleigh–Taylor instabilities form once elastic deformation ceases and plastic yielding occurs.

4. Topographic response from the classical Rayleigh–Taylor instability

The ductile detachment of a portion of the mantle lithosphere (Rayleigh-Taylor instability) may result in opposing topographic response arising from (1) intra-continental orogeny and (2) intra-continental basin formation.

(1) A large number of publications describing various aspects of the Rayleigh–Taylor instability of mantle lithosphere observe negative surface deflection above the dripping "blob" (i. e.: Conrad, 2000; Elkins-Tanton, 2007; Elkins-Tanton and Hager, 2000; Houseman and Molnar, 1997; Le Pourhiet et al., 2006; McKenzie, 1977; Pysklywec and Beaumont, 2004; Saleeby and Foster, 2004). Houseman and Molnar (1997) described the eventual collapse of topography caused by lithospheric extension after detachment of the downwelling lithosphere. Elkins-Tanton (2007) suggested that the buoyant crust significantly limits the topographic depression otherwise created by the sinking and removal of dense lithospheric material. Without buoyant crust and in the presence of large concentrations of dense material the topographic deviations from a zero datum can extend to hundreds of metres.

(2) Neil and Houseman (1999) investigated the role of the Rayleigh–Taylor instabilities in the upper mantle on intra-continental orogeny using numerical models with uniform viscosities and densities as well as the assumption of a Newtonian rheology. Their work showed that positive topographic deflection may occur in a continental lithospheric environment with a thick, buoyant crust. This is sufficient to thicken a 35 km crust to 50 km and produce a significant intraplate mountain range. Buoyant continental crust causes the instability to occur at a lateral wavelength of the order of 300 km regardless of whether a stress-free or rigid condition is used on the upper boundary.

Pysklywec and Beaumont (2004) studied the influence of crustal radioactive heating within the lower crust on the dynamic evolution of topography during the development of Rayleigh–Taylor instabilities, and concluded that there is a feedback between thermal–mechanical processes during the evolution of the radioactive crust in response to a driving mantle downwelling event. This feedback can cause the crust to evolve through phases of: (a) dynamic subsidence of strong crust, potentially forming intracratonic sedimentary basins; (b) flow-induced contraction, thickening and uplift of the self-heating crust; and (c) orogenic deflation as spontaneous crustal extension/thinning and surface subsidence occur. This study has particular implications for regions of high radioactive heat production and juvenile crust, which would more likely have a higher concentration of radioactive elements in the lower crust.

In the numerical experiments presented in this paper, both of the described phenomena above are observed, and are controlled by the nature of the continental crust, as described by the previously mentioned authors. In the model topography responds to the thickness of continental crust above the perturbation. In cases where the initial perturbation is only imposed on mantle lithosphere (Fig. 3, column a), the sinking of the perturbation depresses surface topography at the axis of the symmetry, resulting in basin subsidence directly above the instability. We illustrate this effect in Fig. 4 where the initial depression of the surface topography is followed by long lasting relaxation, leading to extension within the lithosphere after delamination. This evolution is particularly expressed by the switch in direction of maximum compression σ_1 as illustrated in Fig. 3a an effect not considered by Houseman and Molnar (1997). The scale of subsidence is dependent on the initial size of the perturbation; in the case presented on Figs. 3a and 4a, the width of the basin is

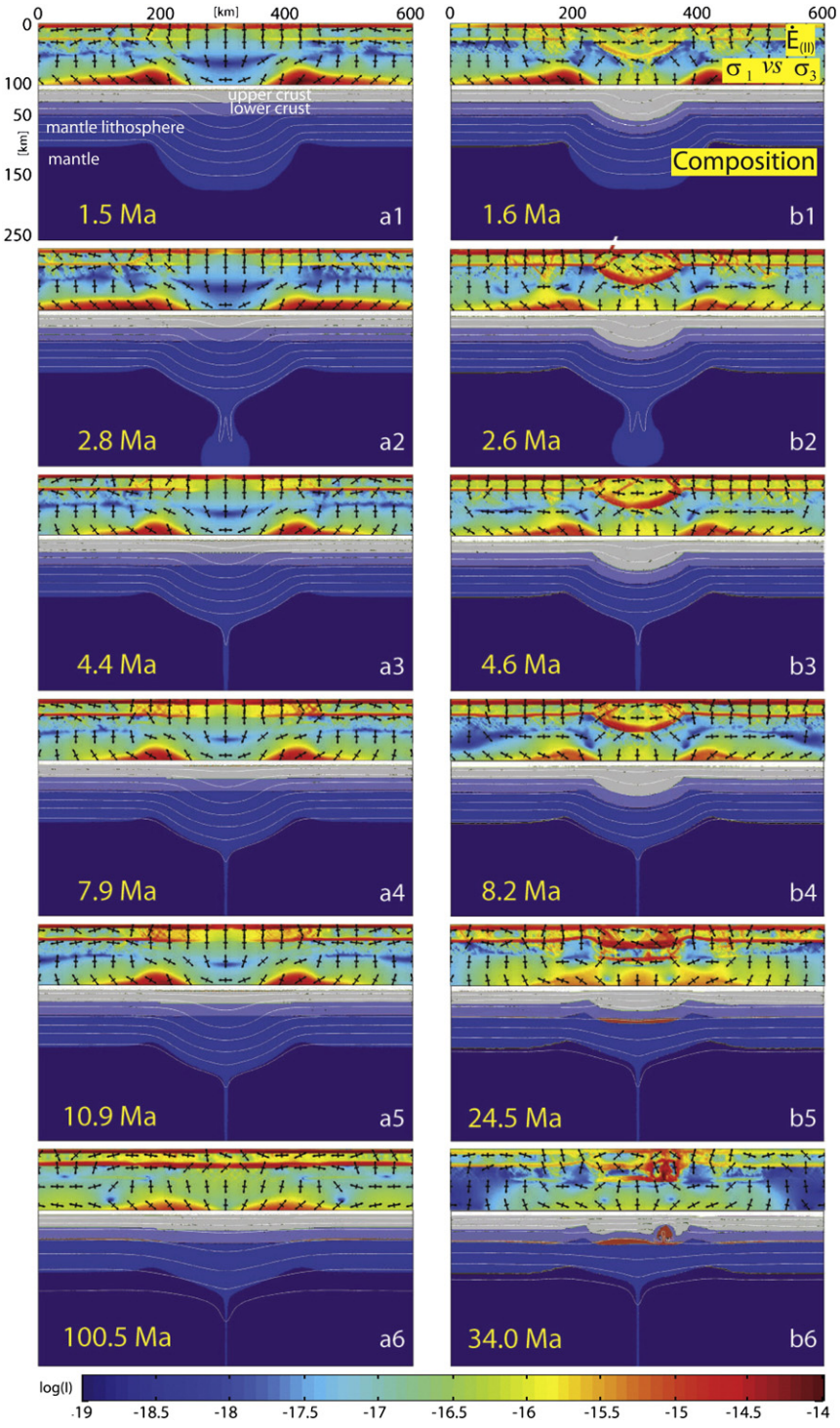

Fig. 3. Dynamic evolution of the lithosphere in two simulations representing different initial geometries: (a) Initial perturbation imposed only on the mantle lithosphere reaching 160 km, initial thickness of the continent is constant across the model. (b) Initial thickness applied to mantle lithosphere (160 km) together with a continental root reaching 80 km. Each time frame is illustrated by two figures: (i) the upper image represents the second strain rate invariant ($\dot{E}_{II}$, colour code) with σ_1 vs σ_3 as black crosses, long axis corresponds to σ_3 and short σ_1; (ii) the lower image shows the composition profile of deformed lithosphere after lapse of indicated time period.

consistent with the initial width of the instability, which in this case has amplitude of 1000 m.

Conversely, when an initial thickness perturbation (a crustal root) is also introduced into a less dense continental crust (continental root), the topographic response differs drastically (Figs. 3b and 4b). The dynamic evolution of the topography can be described in three stages. The initial stage is characterized by uplift (250 m) at the axis of the perturbation as a result of isostatic equilibration within the crust. In the second stage, strong subsidence (100 m) approximately centred along the axis of symmetry occurs, which leads to the formation of basins on the sides of the elevated plateau situated above the instability. At the same time, within the plateau area, subtle subsidence takes place in response to downward displacements arising from the dripping blob. After detachment of the downwelling material, the isostatic rebound of the mantle lithosphere takes place (stage 3). During this stage the temperature at the base of the continental root increases, causing the melting of the lower continental crust. This crustal melting triggers igneous intrusions, volcanic activity at

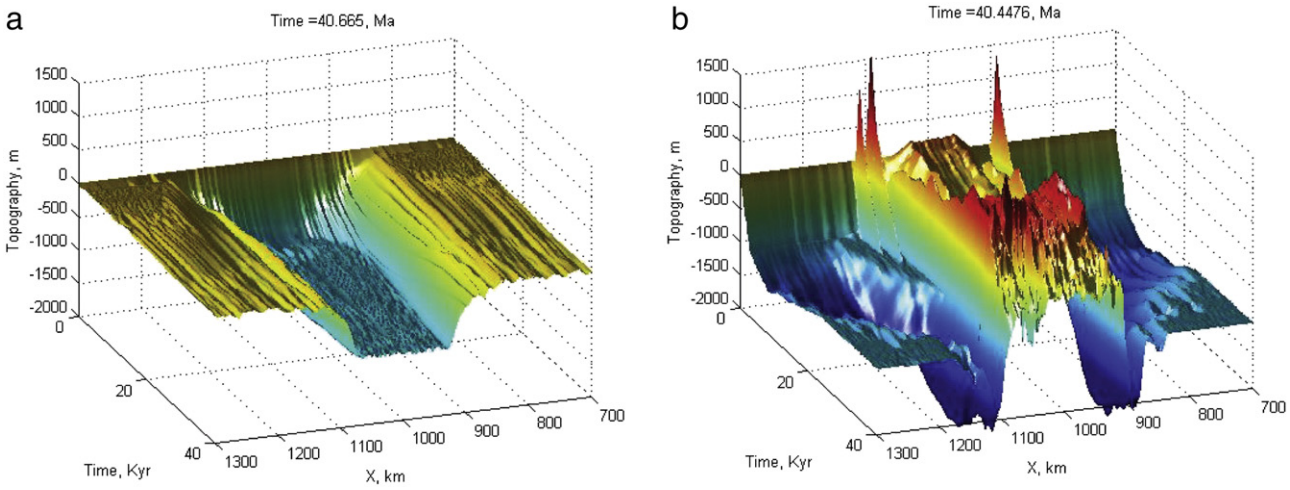

Fig. 4. Dynamic evolution of the topography above the developing instability corresponding to the runs shown in Fig. 3: (a) Run with initial perturbation imposed only on mantle lithosphere; and (b) Run with initial perturbation imposed on whole lithosphere but with additional continental root. The initial peeks in topography on the sides of instability occur due to initial equilibration of topography. Further in the run peaks above the downwelling correspond to intrusion of the magma in to the crust, as well as mountain building processes as a result of deep lithospheric detachment.

the surface and mountain belts. After the main uplift in the axial area, further subsidence (~2 km) takes place, expressed as the development of basins on the sides of the plateau.

5. Melting and the Rayleigh–Taylor instability

Since at least the 1960s, many studies have invoked strong thermal anomalies (mantle plumes) as the main cause of large volume igneous activity in intra-continetal settings (i. e.:Morgan, 1971; Wilson, 1963). However in the last 10 years new concepts have developed. One of these concepts attributes melting to crustal delamination (Lustrino, 2005), where the delamination and sinking of large portions of lower continental crust allow the influx of asthenosphere from the low velocity zone. This ultimately leads to the melts that form the magma source for continental flood basalts. In a concept proposed by Elkins-Tanton (2007), sinking instabilities may devolatilize (similar to what a descending slab in a subduction zone does), and may themselves also melt, or they may carry volatiles to depth, depending upon their sinking rate. Volatiles released into the mantle may be stabilized in solid phases or may trigger melting, even in cases where no dry adiabatic melting is triggered by convection around the sinking instability. Kimberlites or rapidly decompressing volatile-rich magmas rising from depth may be created through this process. Harig et al. (2010) suggested that crystalline plasticity could provide a mechanism for the narrow zones of thinning and upwelling, which would facilitate decompression, and related volcanism far from plate boundaries.

All three the authors cited above suggested that the melting of the mantle lithosphere arises from decompression melting or lowering of the solidus of the mantle by the introduction of fluids from hydrated and detached material, or hydrous heterogeneities that remained after long-gone subduction. Numerical simulations presented in this paper show no melting of mantle lithosphere/asthenosphere as a response to delamination. All of the simulations presented here have used dry olivine rheology for the mantle. As such, no hydrous melting is possible. In addition, no decompression melting of mantle lithosphere and no wholesale detachment of continental lithosphere are observed. On the other hand, these simulations suggest that after the detachment and sinking of cold, dense materials, the elastic rebound of the remaining lithosphere occurs. In response the Moho depth decrease (pressure decreases) and temperature increases in the previously thickened part of the crust. In response to this process melting of lower crust at the base of Moho occurs. This may further result in extensive volcanic activity as well as the extensive emplacement of granitic intrusions, depending on the bulk compositions of the lower crust.

Houseman et al. (1981) and Molnar et al. (1993) have suggested that replacement of lower lithosphere by hot asthenosphere is responsible for rapid heat transfer to and melting of the crust, which may represent another mechanism that leads to melting of the lower crust in intercontinental setting.

6. How to trigger the Rayleigh–Taylor instabilities in intra-plate settings?

All of the models presented in the sections above involve an explicit assumption that sufficient initial stress variations at the base of the lithosphere are introduced by a sufficiently large perturbation in topography at a suitable wavelength, at the base of the lithosphere and/or at the base of the crust (Houseman and Molnar, 1997), or by density increase due to metamorphic processes (Kay and Kay, 1993). Furthermore, the growth rate of the instability must outpace thermal diffusion of the cold mantle lithosphere root into the hot mantle. A question arises at this point: *what process may trigger sufficient large topographic perturbations and/or metamorphic processes in intra-plate regions far away from plate boundaries*?

4-D Lithosphere Mapping methodology (O'Reilly and Griffin, 1996), seismic tomography (Begg et al., 2009) and the analyses of mantle-derived peridotite xenoliths (Griffin et al., 2009) have unveiling secrets hidden beneath continental crust. Careful petrological and seismological studies conducted on the sub-continental lithospheric mantle (SCLM) of Africa, Northern America and Siberia (Griffin et al., 2003; Griffin et al., 2009; O'Neill et al., 2008) indicate that the SCLMs underneath these continents are composed of blocks with different thermal and compositional characteristics, due to strong depletion or extensive metasomatism during tectonic processes such as subduction and/or accretion.

Studies conducted by Djomani et al. (2001) suggested that Archean SCLM sections are significantly buoyant relative to asthenosphere under any reasonable geological scenarios. Given such buoyancy, Archean SCLM cannot be delaminated by gravitational processes alone. Proterozoic SCLM is less depleted and therefore denser (at the same temperature) than Archean SCLM. Thin Proterozoic SCLM (less than about 120 km thick) is denser than the asthenosphere and would be gravitationally unstable. However, Proterozoic lithospheric sections are typically 150 to 180 km thick; such SCLM columns are moderately

buoyant and, like Archean SCLM, are unlikely to be delaminated. Lithospheric sections become gravitationally unstable once they cool down to a steady state conductive geotherm, and then delamination may take place. In these terms only Phanerozoic lithosphere may delaminate in a purely gravitational manner. Another question arises on how to recycle Archean and Proterozoic SCLM. Rifting may represent one explanation, which may allow SCLM disruption and replacement by the upwelling of more fertile asthenospheric (or plume) material (Begg et al., 2009).

Two remaining questions are: 1) how to initiate mechanical thickening of mantle lithosphere far form plate boundaries; and 2) what processes lead to intra-cratonic orogenies and basin formation in a compressional regime?

Taking into consideration that the seismic structure of the lithosphere is heterogeneous and has strong vertical and lateral variations in rheological properties (Begg et al., 2009), we have constructed numerical experiments with simple geometries but with structural heterogeneities to study the influence of such heterogeneities in the lithosphere. Fig. 5a shows the results of four numerical models, which simulate fracture or suture zones by the incorporation of weak zones in the continental lithosphere (such weak zones may have been inherited from the amalgamation of lithospheric blocks, post-collisional structure). Figs. 5b, c and 6 illustrate the behaviour of the continental lithosphere after 20 million years of lithospheric shortening at rate of 2 cm/yr. The results show that lateral heterogeneityies (weak zone) are necessary for the initiation of a perturbation and development of shear zones of lithospheric and crustal scales. In run 1 (Fig. 5) laterally homogenous lithosphere after being subjected to compressional forces did not develop strain localization. Thus occurrence of horizontal weak zone allows for immediate localization of strain. More specifically, from the three models with lateral inhomogeneities (Fig. 5) two (run 2 and 4) develop perturbation at the base of mantle lithosphere that may lead to destabilization and consequently Rayleigh–Taylor. Introducing weak zone through whole lithopshere (run 4) results in the deepest perturbation of cold lithosphere into the asthenosphere — 60 km (Fig. 6). This depth of perturbation is sufficient for the development of a Rayleigh–Taylor instability, as presented in Model 1 (Fig. 3). Run 2 with heterogeneity introduced only in to the mantle lithosphere results in a shallower perturbation of 40 km (Fig. 6), but with a large enough wavelength, an issue addressed by Houseman and Molnar (1997), essential for destabilization of the system.

Sufficient thickening of the lithospheric mantle leads to delamination of the lowers portion of the lithosphere (Fig. 7b), and as expected form previous set of runs the topographic response to delamination is positive, due to thickening of the crustal material, as well and lithospheric mantle. It can be observed that the maximal topographic relief occurs when lithospheric perturbation reaches it's maximum before delamination (Fig. 7c). Interestingly, in the later stage of the run – 25 to 30 Ma the localization of the strain in the crust is focused mainly on crustal scale structures, what may be important for fluid transfer from the mantle lithosphere to the upper crust.

7. Conclusions

The results of our fully coupled geodynamic modelling have demonstrated that the presence of lateral rheological heterogeneities in continental lithosphere may be a crucial component in intra-plate deformation. The existence of such blocky heterogeneity structure in continental lithosphere can be explained by the amalgamation of

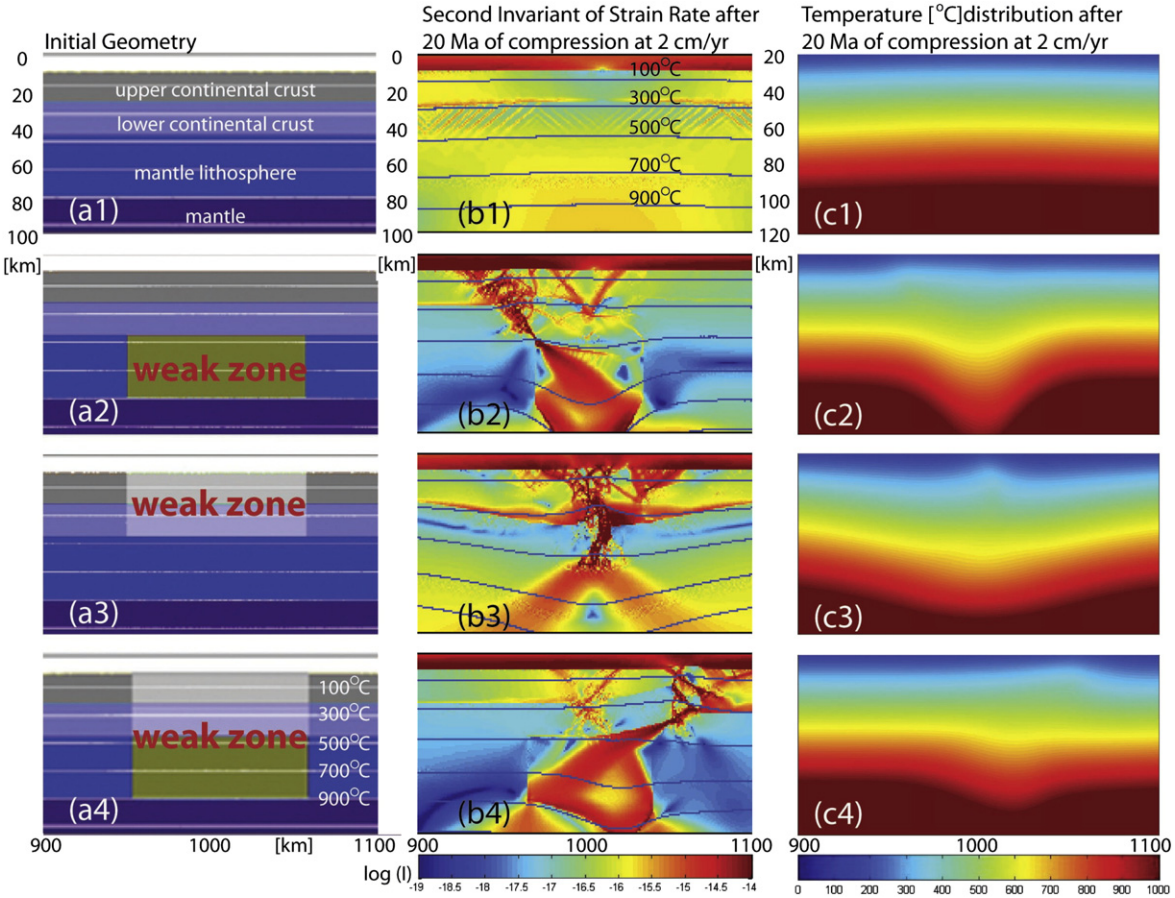

Fig. 5. Results of four models with different initial geometries that are : (a) initial geometry and bulk composition and (b) — second strain rate invariant after 20 Ma of compression at rate of 2 cm/a; (c) temperature distribution after period of 20 Ma.

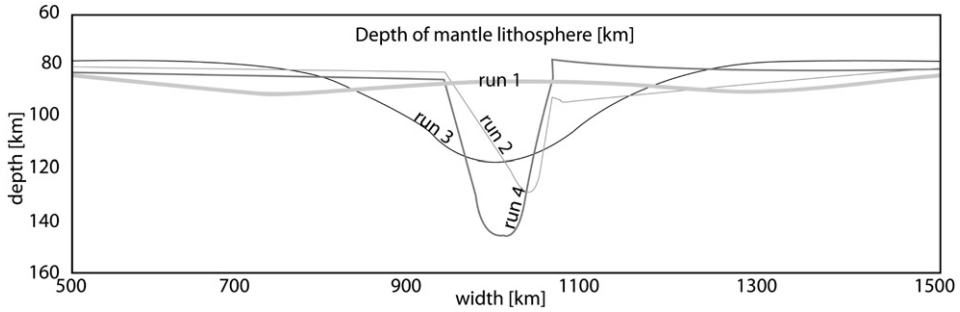

Fig. 6. Depth of the base of the mantle lithosphere after 20 Ma of compression with a rate of 2 cm/yr. The numbering of the curves corresponds to runs presented in Fig. 5.

microplates to the main continent, such as what have been reported for Africa (Begg et al., 2009) and Australia(i. e.:Hand and Sandiford, 1999). Numerical experiments illustrate that lateral variation in rheological properties of rocks may be sufficient to nucleate the perturbation required for the initiation of gravitational instability within SCLM.

Our numerical results are particularly consistent with the observation for Central Australia. The deep seismic profiles in central Australia show that the present day crustal architecture there is the product of amalgamation between the crust and Mesoproterozoic terrane (1100 Ma, Korsch et al., 1998). Reactivation of the post-amalgamation sutures took place at a later stage. Central Australia

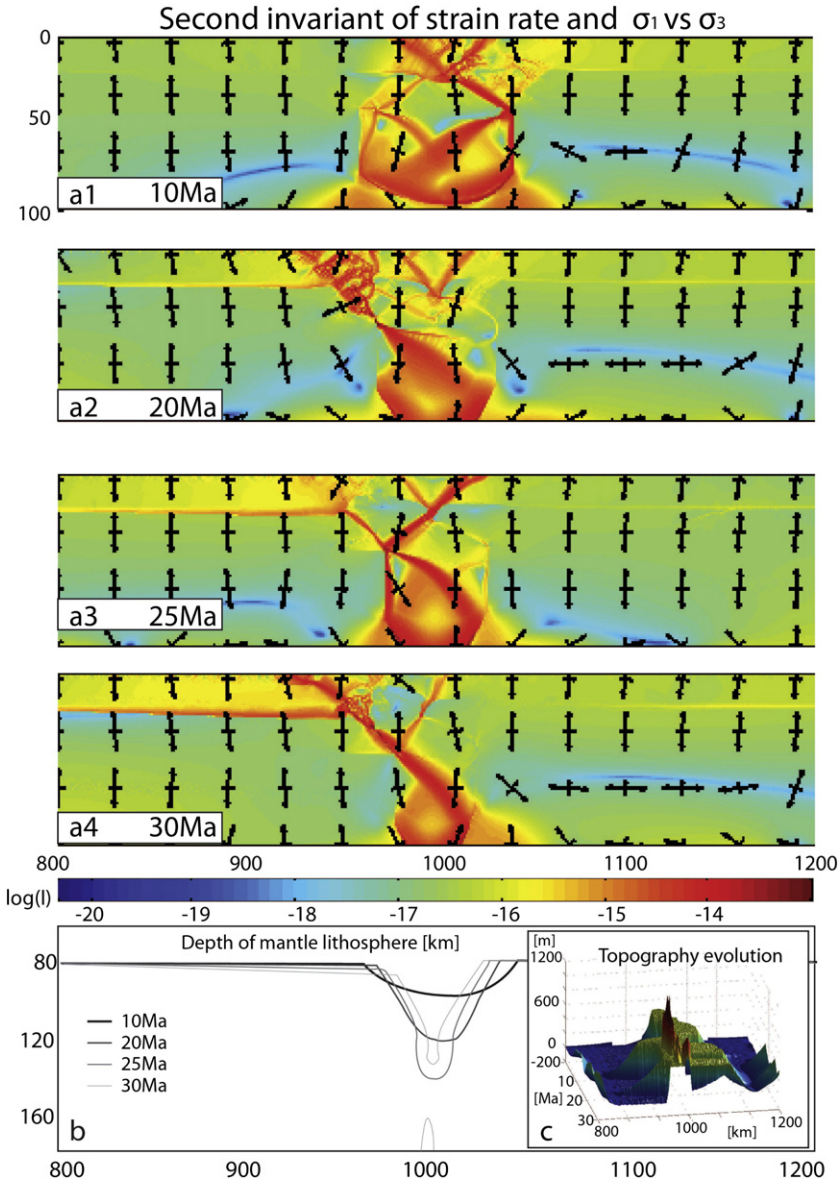

Fig. 7. (a) Second strain rate invariant ($\dot{E}_{II}$, colour code) with σ_1 vs σ_3 as black crosses, long axis corresponds to σ_3 and short σ_1 of the run 4 presented in Fig. 5, (b) evolution of the base of the mantle lithosphere (delamination process), and (c) dynamic evolution of the topography above the developing instability.

underwent Neoproterozoic to Phanerozoic intraplate deformation associated with the formation of the Petermann and Alice Springs Orogens (Sandiford and Hand, 1998). The onset of theses two intraplate orogenies and formation of massive basins in their vicinity may be the result of strong lateral heterogeneities in bulk rock rheology. This led to the localization of deformation/orogeny in suture areas and basin formation on the flanks during the development of SCLM perturbations and delamination. A number of processes may have triggered melting in these regions: decompression (Harig et al., 2010), devolatization of the sinking material (Elkins-Tanton, 2007), melting at the Moho due to thermal equilibration (this study), as well as radical topographic responses (subsidence or uplift). These all indicate that delamination of mantle lithosphere in intra-continental settings is a very complex process, comparable in complexity to processes at the boundary of the plates.

Acknowledgements

This work was financially supported by CSIRO and AuScope. Constructive review by Peter Molnar and Manuele Faccenda is greatly appreciated.

Reference

Anderson, D.L., 1995. Lithosphere, asthenosphere, and perisphere. Reviews of Geophysics 33 (1), 125–149.
Begg, G.C., Griffin, W.L., et al., 2009. The lithospheric architecture of Africa: seismic tomography, mantle petrology, and tectonic evolution. Geosphere 5 (1), 23–50.
Bird, P., 1978. Initiation of intracontinental subduction in Himalaya. Journal of Geophysical Research 83 (NB10), 4975–4987.
Bird, P., 1979. Continental delamination and the Colorado Plateau. Journal of Geophysical Research 84 (NB13), 7561–7571.
Bittner, D., Schmeling, H., 1995. Numerical modeling of melting processes and induced diapirism in the lower crust. Geophysical Journal International 123 (1), 59–70.
Brace, W.F., Kohlstedt, D.L., 1980. Limits on lithospheric stress imposed by laboratory experiments. Journal of Geophysical Research 85 (NB11), 6248–6252.
Buick, I.S., Close, D., et al., 2001. High-pressure melting and fluid flow during the Petermann Orogeny, central Australia. Water-Rock Interaction 1 and 2, 677–680.
Burg, J.P., Gerya, T.V., 2005. The role of viscous heating in Barrovian metamorphism of collisional orogens: thermomechanical models and application to the Lepontine Dome in the Central Alps. Journal of Metamorphic Geology 23 (2), 75–95.
Calais, E., Han, J.Y., et al., 2006. Deformation of the North American plate interior from a decade of continuous GPS measurements. Journal of Geophysical Research 111 (B6), B06402.
Calais, E., Mattioli, G., et al., 2005. Seismology: tectonic strain in plate interiors? Nature 438 (7070), E9–E10.
Christensen, U.R., Yuen, D.A., 1985. Layered convection induced by phase-transitions. Journal of Geophysical Research-Solid Earth and Planets 90 (NB12), 291–300.
Clauser, C., Huenges, E., 1995. Thermal conductivity of rocks and minerals. Rock physics and phase relations. In: Ahrens, T.J. (Ed.), Washington, D.C., American Geophysical Union Reference Shelf, 3, pp. 105–126.
Connolly, J.A.D., Kerrick, D.M., 2002. Metamorphic controls on seismic velocity of subducted oceanic crust at 100–250 km depth. Earth and Planetary Science Letters 204 (1–2), 61–74.
Conrad, C.P., 2000. Convective instability of thickening mantle lithosphere. Geophysical Journal International 143 (1), 52–70.
Conrad, C.P., Molnar, P., 1999. Convective instability of a boundary layer with temperature- and strain-rate-dependent viscosity in terms of 'available buoyancy'. Geophysical Journal International 139 (1), 51–68.
Craddock, J.P., van der Pluijm, B.A., 1999. Sevier-Laramide deformation of the continental interior from calcite twinning analysis, west-central North America. Tectonophysics 305 (1–3), 275–286.
Djomani, Y.H.P., O'Reilly, S.Y., et al., 2001. The density structure of subcontinental lithosphere through time. Earth and Planetary Science Letters 184 (3–4), 605–621.
Dyksterhuis, S., Muller, R.D., 2008. Cause and evolution of intraplate orogeny in Australia. Geology 36 (6), 495–498.
Elkins-Tanton, L.T., 2007. Continental magmatism, volatile recycling, and a heterogeneous mantle caused by lithospheric gravitational instabilities. Journal of Geophysical Research-Solid Earth 112 (B3).
Elkins-Tanton, L.T., Hager, B.H., 2000. Melt intrusion as a trigger for lithospheric foundering and the eruption of the Siberian flood basalts. Geophysical Research Letters 27 (23), 3937–3940.
Elliott, T., Plank, T., et al., 1997. Element transport from slab to volcanic front at the Mariana arc. Journal of Geophysical Research-Solid Earth 102 (B7), 14991–15019.
Gerya, T., 2010. Introduction to Numerical Geodynamic Modelling. Cambridge University Press.
Gerya, T.V., Connolly, J.A.D., et al., 2008. Why is terrestrial subduction one-sided? Geology 36 (1), 43–46.
Gerya, T.V., Yuen, D.A., 2007. Robust characteristics method for modelling multiphase visco-elasto-plastic thermo-mechanical problems. Physics of the Earth and Planetary Interiors 163 (1–4), 83–105.
Gorczyk, W., Gerya, T.V., et al., 2007. Melting and mixing processes in mantle wedges. Geochimica Et Cosmochimica Acta 71 (15), A346–A.
Griffin, W.L., O'Reilly, S.Y., et al., 2003. The origin and evolution of Archean lithospheric mantle. Precambrian Research 127 (1–3), 19–41.
Griffin, W.L., O'Reilly, S.Y., et al., 2009. The composition and evolution of lithospheric mantle: a re-evaluation and its tectonic implications. Journal of Petrology 50 (7), 1185–1204.
Hand, M., Sandiford, M., 1999. Intraplate deformation in central Australia, the link between subsidence and fault reactivation. Tectonophysics 305 (1–3), 121–140.
Harig, C., Molnar, P., et al., 2010. Lithospheric thinning and localization of deformation during Rayleigh–Taylor instability with nonlinear rheology and implications for intracontinental magmatism. Journal of Geophysical Research 115.
Hawkesworth, C.J., Turner, S.P., et al., 1997. U–Th isotopes in arc magmas: implications for element transfer from the subducted crust. Science 276 (5312), 551–555.
Hoogenboom, T., Houseman, G.A., 2006. Rayleigh–Taylor instability as a mechanism for corona formation on Venus. Icarus 180 (2), 292–307.
Houseman, G., McKenzie, D.P., 1982. Numerical experiments on the onset of convective instability in the earths mantle. Geophysical Journal of the Royal Astronomical Society 68 (1), 133–164.
Houseman, G.A., McKenzie, D.P., et al., 1981. Convective instability of a thickened boundary-layer and its relevance for the thermal evolution of continental convergent belts. Journal of Geophysical Research 86 (NB7), 6115–6132.
Houseman, G.A., Molnar, P., 1997. Gravitational (Rayleigh–Taylor) instability of a layer with non-linear viscosity and convective thinning of continental lithosphere. Geophysical Journal International 128 (1), 125–150.
Ingersoll, R.V., 1988. Tectonics of sedimentary basins. Geological Society of America Bulletin 100 (11), 1704–1719.
Jordan, T.H., 1978. Composition and development of the continental tectosphere. Nature 274 (5671), 544–548.
Jull, M., Kelemen, P.B., 2001. On the conditions for lower crustal convective instability. Journal of Geophysical Research-Solid Earth 106 (B4), 6423–6446.
Kay, R.W., Kay, S.M., 1993. Delamination and delamination magmatism. Tectonophysics 219 (1–3), 177–189.
Kerrick, D.M., Connolly, J.A.D., 2002. Quantification of subduction zone metamorphic devolatilization from computed high pressure phase equilibria. Geochimica Et Cosmochimica Acta 66 (15A), A396-A396.
Kevin, B., 1976. The chad basin: an active intra-continental basin. Tectonophysics 36 (1–3), 197–206.
Korsch, R.J., Goleby, B.R., et al., 1998. Crustal architecture of central Australia based on deep seismic reflection profiling. Tectonophysics 288 (1–4), 57–69.
Le Pourhiet, L., Gurnis, M., et al., 2006. Mantle instability beneath the Sierra Nevada Mountains in California and Death Valley extension. Earth and Planetary Science Letters 251 (1–2), 104–119.
Lev, E., Hager, B.H., 2008. Rayleigh–Taylor instabilities with anisotropic lithospheric viscosity. Geophysical Journal International 173 (3), 806–814.
Lustrino, M., 2005. How the delamination and detachment of lower crust can influence basaltic magmatism. Earth-Science Reviews 72 (1–2), 21–38.
McKenzie, D., 1977. Surface deformation, gravity anomalies and convection. Geophysical Journal of the Royal Astronomical Society 48 (2), 211–238.
Molnar, P., England, P., et al., 1993. Mantle dynamics, uplift of the Tibetan Plateau, and the Indian Monsoon. Reviews of Geophysics 31 (4), 357–396.
Molnar, P., Houseman, G.A., et al., 1998. Rayleigh–Taylor instability and convective thinning of mechanically thickened lithosphere: effects of non-linear viscosity decreasing exponentially with depth and of horizontal shortening of the layer. Geophysical Journal International 133 (3), 568–584.
Moore, D.E., Lockner, D.A., et al., 1997. Strengths of serpentinite gouges at elevated temperatures. Journal of Geophysical Research-Solid Earth 102 (B7), 14787–14801.
Morgan, W.J., 1971. Convection plumes in lower mantle. Nature 230 (5288), 42–43.
Neil, E.A., Houseman, G.A., 1999. Rayleigh–Taylor instability of the upper mantle and its role in intraplate orogeny. Geophysical Journal International 138 (1), 89–107.
O'Neill, C.J., Lenardic, A., et al., 2008. Dynamics of cratons in an evolving mantle. Lithos 102 (1–2), 12–24.
O'Reilly, S.Y., Griffin, W.L., 1996. 4-D lithosphere mapping: methodology and examples. Tectonophysics 262 (1–4), 3–18.
Piriz, A.R., Cela, J.J.L., et al., 2009. Rayleigh–Taylor instability in elastic–plastic solids. Journal of Applied Physics 105 (11).
Poudjom Djomani, Y.H., O'Reilly, S.Y., et al., 2001. The density structure of subcontinental lithosphere through time. Earth and Planetary Science Letters 184 (3–4), 605–621.
Pysklywec, R.N., Beaumont, C., 2004. Intraplate tectonics: feedback between radioactive thermal weakening and crustal deformation driven by mantle lithosphere instabilities. Earth and Planetary Science Letters 221 (1–4), 275–292.
Ranalli, G., 1995. Rheology of the Earth. Chapman and Hall, London.
Saleeby, J., Foster, Z., 2004. Topographic response to mantle lithosphere removal in the southern Sierra Nevada region, California. Geology 32, 245–248.
Sandiford, M., Hand, M., 1998. Controls on the locus of intraplate deformation in central Australia. Earth and Planetary Science Letters 162 (1–4), 97–110.
Sandiford, M., Quigley, M., et al., 2009. Tectonic framework for the Cenozoic cratonic basins of Australia. Australian Journal of Earth Sciences 56, 5–18.
Schmidt, M.W., Poli, S., 1998. Experimentally based water budgets for dehydrating slabs and consequences for arc magma generation. Earth and Planetary Science Letters 163, 361–379.

Schott, B., Schmeling, H., 1998. Delamination and detachment of a lithospheric root. Tectonophysics 296 (3–4), 225–247.
Stephenson, R., Egholm, D.L., et al., 2009. Role of thermal refraction in localizing intraplate deformation in southeastern Ukraine. Nature Geoscience 2 (4), 290–293.
Turcotte, D.L., Schubert, G., 2002. Geodynamics. Cambridge University Press, Cambridge.
Wilson, J.T., 1963. A possible origin of Hawaiian Islands. Canadian Journal of Physics 41 (6), 863–870.
Ye, H., Shedlock, K.M., et al., 1985. The North China basin: an example of a Cenozoic rifted intraplate basin. Tectonics 4 (2), 153–169.